

SEMIANNUAL TECHNICAL REPORT NUMBER ONE

AD 735645

ARPA Order Number: 1579, Amendment 2
Program Code Number: 1F10
Contractor: Southwest Research Institute
Effective Date of Contract: March 5, 1971
Contract Expiration Date: April 4, 1972
Amount of Contract: \$61,131
Contract Number: H0210036
Principal Investigator: U. S. Lindholm 512/684-5111
Project Engineer: Same
Title: A Study of the Dynamic Strength and Fracture Properties of Rock

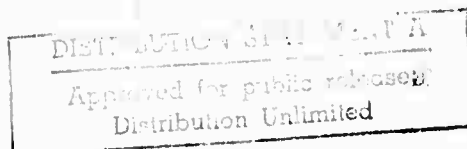
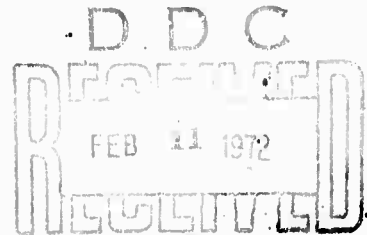
Sponsored by

Advanced Research Projects Agency
ARPA Order No. 1579, Amend. 2
Program Code 1F10

This research was supported by the Advanced Research Projects Agency of the Department of Defense and was monitored by the Bureau of Mines under Contract No. H0210036.

The views and conclusions contained in this document are those of the authors and should not be interpreted as necessarily representing the official policies, either expressed or implied, of the Advanced Research Projects Agency or the U. S. Government.

Reproduced by
NATIONAL TECHNICAL
INFORMATION SERVICE
Springfield, Va 22151



**BEST
AVAILABLE COPY**

DOCUMENT CONTROL DATA - R & D

(Security classification of title, body of abstract and indexing annotation must be entered when the overall report is classified)

1. ORIGINATING ACTIVITY (Corporate author) Southwest Research Institute P. O. Drawer 28510 San Antonio, Texas 78284		2a. REPORT SECURITY CLASSIFICATION UNCLASSIFIED	
		2b. GROUP	
3. REPORT TITLE A Study of the Dynamic Strength and Fracture Properties of Rock			
4. DESCRIPTIVE NOTES (Type of report and inclusive dates) Semiannual Technical Report Number One			
5. AUTHOR(S) (First name, middle initial, last name) Ulric S. Lindholm			
6. REPORT DATE 4 February 1972		7a. TOTAL NO. OF PAGES 22	7b. NO. OF REFS 6
8a. CONTRACT OR GRANT NO. H0210036		9a. ORIGINATOR'S REPORT NUMBER(S) 02-3092 No. 1	
b. PROJECT NO. ARPA Order No. 1579, Amend. 2			
c. Program Code 1F10		9b. OTHER REPORT NO(S) (Any other numbers that may be assigned this report)	
d.			
10. DISTRIBUTION STATEMENT Distribution of this document is unlimited.			
11. SUPPLEMENTARY NOTES		12. SPONSORING MILITARY ACTIVITY Advanced Research Projects Agency, Department of Defense, Bureau of Mines	
13. ABSTRACT The objective of this program is to determine the effect of strain rate ($10^{-4} - 10^4 \text{sec}^{-1}$), temperature ($80^\circ - 800^\circ \text{K}$) and confining pressure (0 - 7 Kbars) on the strength properties of hard rock. Compression tests have been performed on Dresser basalt using hydraulic test equipment at the lower rates and Hopkinson pressure bar apparatus at the highest rates. Test results are presented which show that the temperature and strain-rate dependence of the fracture stress is described by a relation of the form $\sigma_f = \sigma_0 - \beta T \log \dot{\epsilon}_0 / \dot{\epsilon}$. This suggests that the fracture process is controlled by some type of thermally activated mechanism. The pressure dependence of the fracture stress obeys a linear, Coulomb-Mohr type criteria. Further tests will be conducted to establish the combined effect of pressure and strain rate on the flow and fracture strength.			

KEY WORDS	LINK A		LINK B		LINK C	
	ROLE	WT	ROLE	WT	ROLE	WT
Rock Mechanics Strain-Rate Effects Fracture						

SUMMARY

The objective of this program is to determine the effect of strain rate ($10^{-4} - 10^4 \text{ sec}^{-1}$), temperature ($80^\circ - 800^\circ \text{K}$) and confining pressure (0 - 7 Kbars) on the strength properties of hard rock. Compression tests have been performed on Dresser basalt using hydraulic test equipment at the lower rates and Hopkinson pressure bar apparatus at the highest rates. Test results are presented which show that the temperature and strain-rate dependence of the fracture stress is described by a relation of the form $\sigma_f = \sigma_0 - \beta T \log \frac{\dot{\epsilon}_0}{\dot{\epsilon}}$. This suggests that the fracture process is controlled by some type of thermally activated mechanism. The pressure dependence of the fracture stress obeys a linear, Coulomb-Mohr type criteria. Further tests will be conducted to establish the combined effect of pressure and strain rate on the flow and fracture strength.

I. RESEARCH OBJECTIVES

Fundamental to the understanding of any mechanical process involving rock is an adequate description of its strength properties. These strength properties may be significantly influenced by a number of loading and environmental parameters. The basic objective of this program is to investigate the effects of temperature and high strain rates on the strength properties of hard rock. At present, there exists very little data on the strength and fracture properties of rock at rates of deformation comparable to those obtained during mechanical drilling (rotary or percussion) or during seismic or shock wave propagation through the earth. Therefore, one objective is to obtain experimental data in this range of interest. Often the ductility or energy required to fracture rock can be sharply influenced by even relatively small changes in temperature, deformation rate, or confining pressure. There is often a relatively abrupt transition from ductile (high fracture energy) to brittle (low fracture energy) behavior. Definition of this transition region is important to those processes requiring comminution of rock with minimum input energy.

While the experimental data will be new and useful in itself, another important objective will be the development of an appropriate and meaningful constitutive relation for the type of rock studied. A starting hypothesis for this development will be the established theory for rate processes controlled

by thermal activation. The range in test variables chosen (temperature and strain rate) is based upon the need to verify this hypothesis as well as to encompass a range of practical interest where relatively little data presently exists.

The proposed approach to the constitutive equation has application to the static and creep properties of rock also. Therefore, its establishment has more general and significant application than just impact problems. It should relate to the basic mechanisms controlling inelastic deformation and fracture. Of course, measurements on the aggregate may reflect a number of mechanisms operating either simultaneously or independently over different ranges of the relevant parameters. It will be attempted to identify as many of these as possible.

II. PROGRAM ORGANIZATION

For purposes of organization, the program effort has been broken up into six technical tasks. A brief description of these tasks is included below:

Task I. Design and Fabrication of Equipment. While all of the major test equipment was available, certain modifications were required for the testing of hard rock. Two different loading facilities are being utilized. At low and intermediate strain rates, a hydraulic ram facility is used which may be operated either closed or open loop depending upon the crosshead (ram) velocity. Maximum velocity (no load) is of the order of 10 in./sec.

The second facility is a split Hopkinson pressure bar device for high rate testing. A test chamber for 100,000 psi confining pressure was adapted for use with both these axial loading facilities. Modification and development of associated instrumentation was also required.

Task II. Selection and Preparation of Rock Specimens. Because of the large number of test parameters, only one rock type is being considered. At the suggestion of the Bureau of Mines, a hard basalt obtained from the Bryan-Dresser Drop Rock Co. in Shakopee, Wisconsin, was selected. This is an intact rock of high strength and relatively fine grain size. Specimen preparation has been by standard core drilling and grinding.

Task III. Low and Intermediate Rate Testing. This task includes all testing on the hydraulic machine. The test data will consist of stress-strain curves to failure with strain rate, temperature, and confining pressure held as constant test parameters. The range for the test parameters is:

Confining pressure	0 - 100,000 psi
Temperature	80° - 800°K
Strain rate	10^{-4} - ≈ 10 sec ⁻¹

While initially it was proposed to test in shear (torsion), tests to date have been in compression. This has proved more economical without sacrificing the technical objectives.

Task IV. High Strain-Rate Tests. This task included all testing with the split Hopkinson bar technique to obtain strain rates in the range from 10^2 to 10^4 sec⁻¹. Confining pressures to at least 20,000 psi and potentially

higher will be included. The high rate tests will include the same range in temperatures as above. In all tests the elevated and reduced temperatures are obtained only for the case of zero confining pressure.

Task V. Examination of Fracture Surfaces. The fractured specimens will be examined to characterize both the gross fracture mode and the microscopic fracture topography. The fracture appearance will be related to the testing conditions for possible indications of the detailed fracture mechanisms involved.

Task VI. Correlation of Test Data. The test data are being examined and correlated with existing theory based upon rate processes. This theory is quite general and has been applied successfully in the past to both deformation and fracture of crystalline and polymeric materials. There is evidence that it will prove applicable for rock.

III. SUMMARY OF TECHNICAL PROGRESS

Specimen Description

The rock selected for testing is a basalt obtained from a quarry in Wisconsin. All specimens have been obtained from a single boulder. The rock is a very hard, mottled black to grey and dull olive green, very fine grained (mostly 20 to 500 micron intergrown crystals, metamorphosed (serpentinized) igneous rock with some larger serpentinized pyroxene crystals distributed throughout. Serpentinization is most thorough in an interconnecting, vein-like network throughout the rock.

Petrographic sections show the rock to be composed of a fine-grained (aphanitic) intergrown ground mass (matrix) of pyroxene, serpentine, plagioclase feldspars (mainly labradorite, bytownite, and andesine), melilite, magnetite, and a little olivine--some with a trace of iddingsite.

An intertwining network of vein-like serpentized (metamorphosed) material is common throughout the rock. The serpentine network outlines some rounded masses (up to 1/4-inch) of rather uniformly sized intergrowths of pyroxene and feldspar containing some melilite. Magnetite and/or ilmenite occurs disseminated on the outer fringes of these ovoidal areas, as well as rather well disseminated throughout the rock. Some larger (up to 1/4- inch) crystals (phenocrysts) of partially serpentized pyroxene occur scattered throughout. The rock can be classed as a serpentized basalt.

Approximate mineral type, percentage composition, and crystal sizes are shown below:

<u>Mineral</u>	<u>Volume</u>	<u>Most Crystals</u>	<u>Largest Crystal</u>
Serpentine	45-60%	20-80 μ	1000 μ
Pyroxene	20-25	20-800	4000
Plagioclase feldspar	10-20	20 to 40- 100 to 240	60 to 480
Magnetite &/or ilmenite	3-5	20-150	900
Melilite (& nephelite?)	3-5	80-120	320
Olivine	< 1	50-200	500
Iddingsite	Tr	20-100	200

The test specimens are nominally 1/2-inch in diameter and 1-inch long. They are obtained by core drilling and grinding of the ends to obtain flatness and parallelism within 0.0002 inch. Specimens were taken from three orthogonal directions in the boulder. Tests with these specimens indicate that the rock is macroscopically isotropic with respect to its strength properties.

Test Equipment and Procedures

The low and intermediate rate tests are being performed with conventional hydraulic test equipment. While it was initially planned to use a 10,000-lb capacity hydraulic actuator for the axial load, the high strength of the Dresser basalt forced us to go to a 50,000-lb actuator. This larger load requirement (piston area) reduces the maximum strain rate obtainable. Results are being obtained in the range from 10^{-4} to 1 sec^{-1} with the larger actuator.

Radial confining pressure is achieved with a 100 ksi pressure chamber. From 0 to 20 ksi we have a servo-programmable intensifier for the radial pressure. From 20 to 100 ksi the intensifier is static and requires recycling. In the future we intend to develop a programmable intensifier for pressures from 0 to 100 ksi. This will allow programming of both the axial and radial load (or strain).

Figure 1 shows the specimen arrangement prior to insertion in the pressure cylinder. The specimen is sealed with thin, heat-shrinkable polyolefin tubing. This tubing allows attachment of the two clip-type extensometers shown in the figure. These extensometers employ strain-gaged flexure arms as the sensing elements. The four attachment points for each extensometer reference directly to the rock surface and are sealed with a gage-coat normally used to seal strain-gages. The two extensometers measure radial (diametral) and axial strain continuously. Strain gages for load measurement are in series with the specimen and within the pressurized area. A correction is made for the pressure sensitivity of the strain gages.

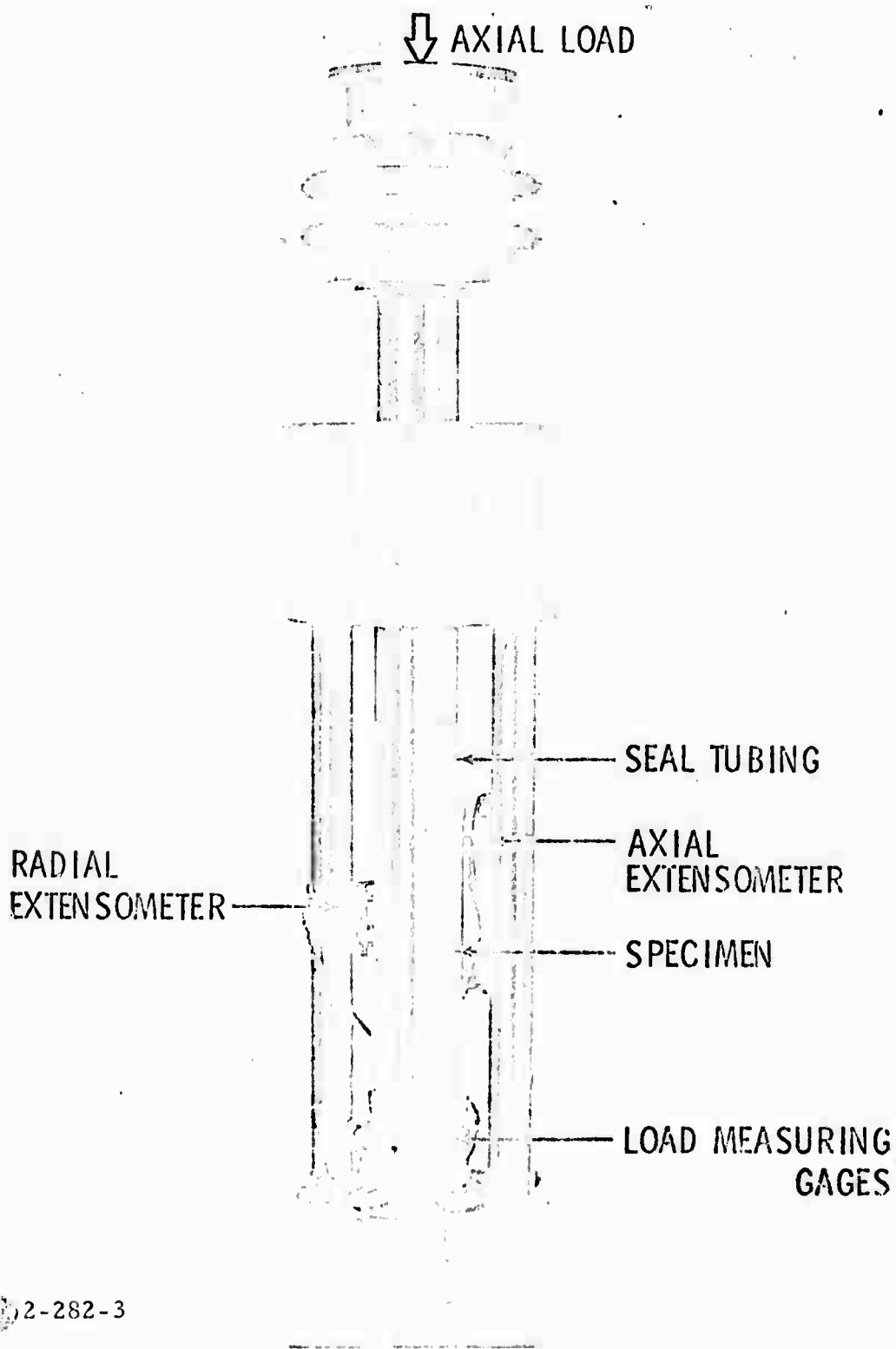


FIGURE 1. SPECIMEN ARRANGEMENT FOR LOW RATE TESTS

A typical record from this system is shown in Figure 2. Two x-y recordings are made: the axial (z) stress versus axial strain, and radial strain versus axial strain. The stress coordinate labeled σ_z is actually the differential stress $\sigma_z - \sigma_R$ or $\sigma_z - P$ where P is the confining pressure. The record of Figure 2 was obtained at $P = 20,000$ psi. Tests under confining pressure are controlled from the radial extensometer. Gross failure of the rock generally occurs at the maximum load and is accompanied by an audible "pop". In some cases, the strain control prevents a large stress drop but generally the failure is brittle and accompanied by a rather sudden energy release. After fracture at maximum load there is multiple faulting and the strain is no longer homogeneous. Therefore, after maximum load is reached the curves are not very repeatable.

For the low temperature tests, the loading anvils adjacent to the specimen were cooled with liquid nitrogen and the specimen brought to thermal equilibrium by conduction. For the high temperature tests the specimen and anvils were heated by radiation from quartz lamps. Temperature control was within $\pm 4^\circ\text{C}$.

Figure 3 shows the split Hopkinson bar apparatus for the high rate tests. A detailed description of this technique has been given by Lindholm^(1,2). It has previously been applied to geologic materials by Green and Perkins⁽³⁾ for unconfined tests.

The system in Figure 3 is newly developed and differs from our previous systems^(1,2) by allowing for higher impact velocity (stress), axial preloading,

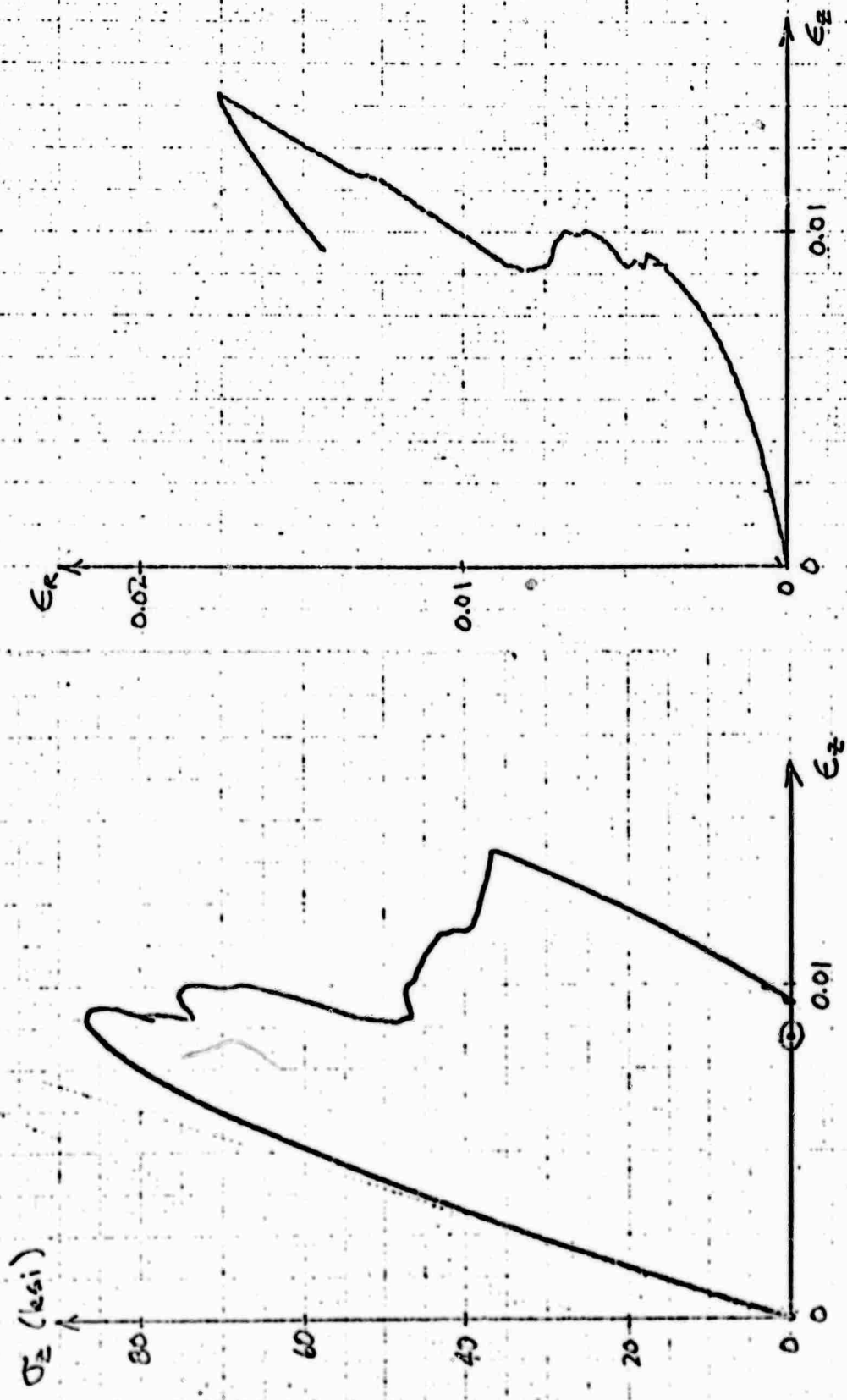


FIGURE 2. TYPICAL RECORD FROM LOW SPEED TEST
($\dot{\epsilon} = 10^{-3} \text{ sec}^{-1}$, $T = 300^\circ\text{K}$, $P = 20 \text{ ksi}$)

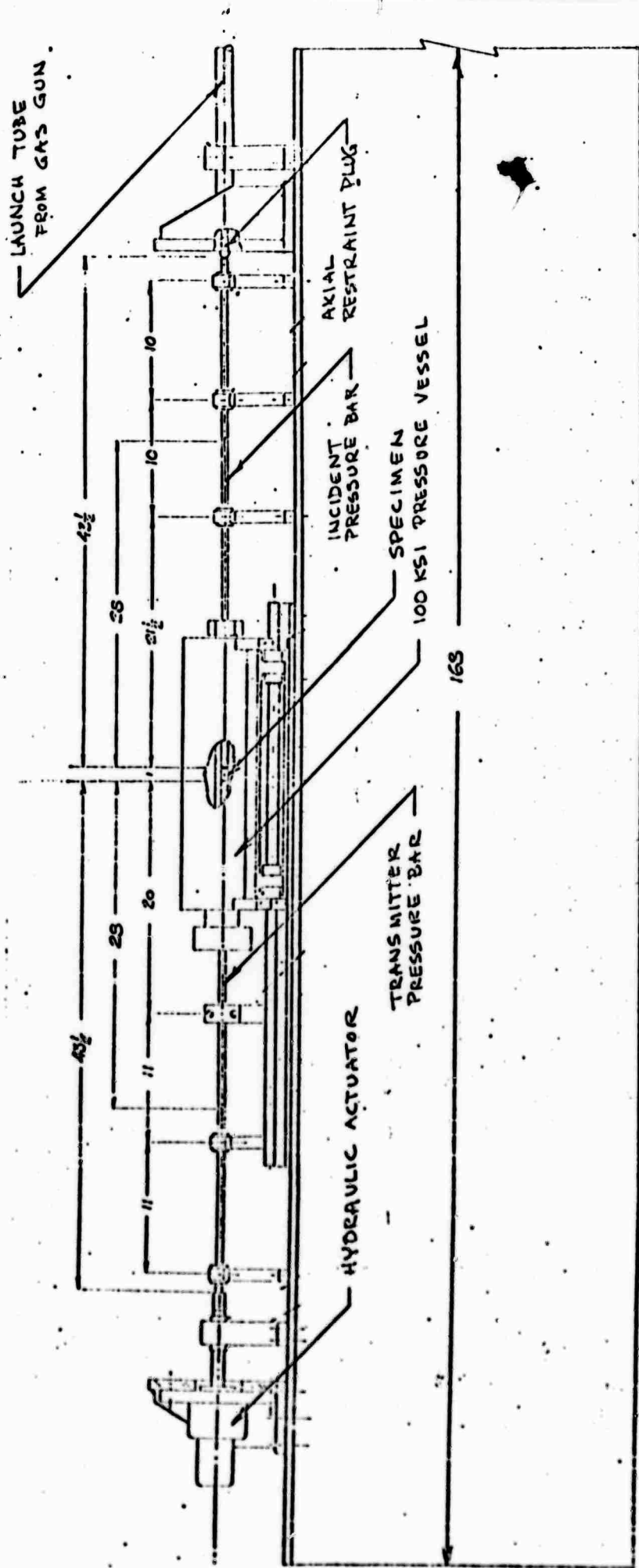


FIGURE 3. SCHEMATIC OF HOPKINSON BAR APPARATUS

and radial confining pressure. The higher velocities and stresses are achieved by using a pneumatically-driven projectile (impacting bar) guided by a long launch tube. Maximum impact velocities are of the order of 2000 in./sec controlled by the maximum yield stress in the pressure bars. These bars are made from a specialty steel tempered to a yield stress of approximately 350,000 psi.

The axial preload is generated by the hydraulic actuator at the far end of the transmitter pressure bar. The axial load generated by this actuator may be servoed to the amplitude of the radial confining pressure to produce hydrostatic loading. The axial load is reacted by an axial restraint plug, having a conical collar, and located at the impact end of the incident pressure bar. The impact is transmitted through this plug.

The 100 ksi pressure vessel surrounds the specimen with the pressure bars entering through packing seals at each end of the vessel. The recording strain gages on the pressure bars are outside the pressure vessel and therefore operate at ambient pressure. The pressure vessel is supported on rails and translates axially to allow access to the specimen.

This facility has been assembled and operated successfully for tests without confining pressure. Tests with confining pressure are the subject of current effort.

Test Results with Dresser Basalt

Approximately 50 tests have been run to date covering most of the range of temperatures, strain rates and confining pressures. Some of this preliminary data is shown in Figures 4, 5 and 6.

Figure 4 illustrates the effect of temperature and of confining pressure on the stress-strain curve. For the unconfined specimens ($P = 0$) there is very little inelastic deformation at any temperature between the test limits of 80° to 300°K . The apparent proportional limit or deviation from linearity is indicated by the slash mark. It will be noted that at temperatures below 300°K the fracture stress increases rapidly with decreasing temperature. The proportional or elastic limit also increases. The stress-strain curves, on the right-hand side of the figure, are all obtained at room temperature (300°K) but with increasing confining pressure. Again there is a sharp increase in fracture stress, however the proportional limit remains nearly constant with pressure. The inelastic strain remains small and of the order of magnitude of the elastic strain even at $P = 75$ ksi.

Figure 5 shows the effect of temperature and strain rate on the fracture stress for the unconfined rock. Three strain rates are included covering a range of seven orders in magnitude. The data shows the usual trends associated with processes which are controlled by thermal activation. The solid lines through the data correspond to the equation

$$\sigma_f = \sigma_0 - \beta T \log \frac{\dot{\epsilon}_f}{\dot{\epsilon}} \quad ; \quad \sigma > 40 \text{ ksi} \quad (1)$$

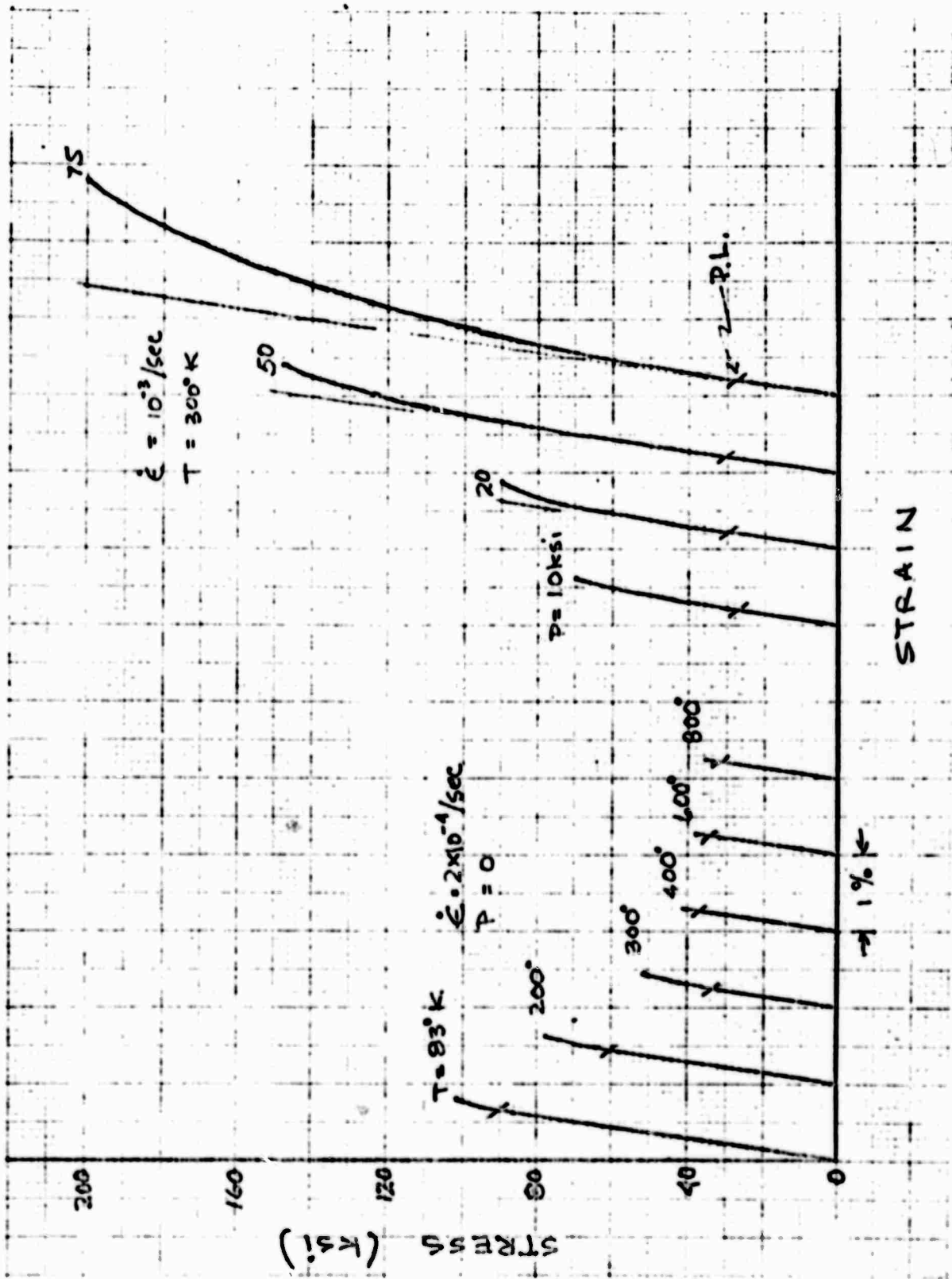


FIGURE 4. TYPICAL STRESS-STRAIN CURVES

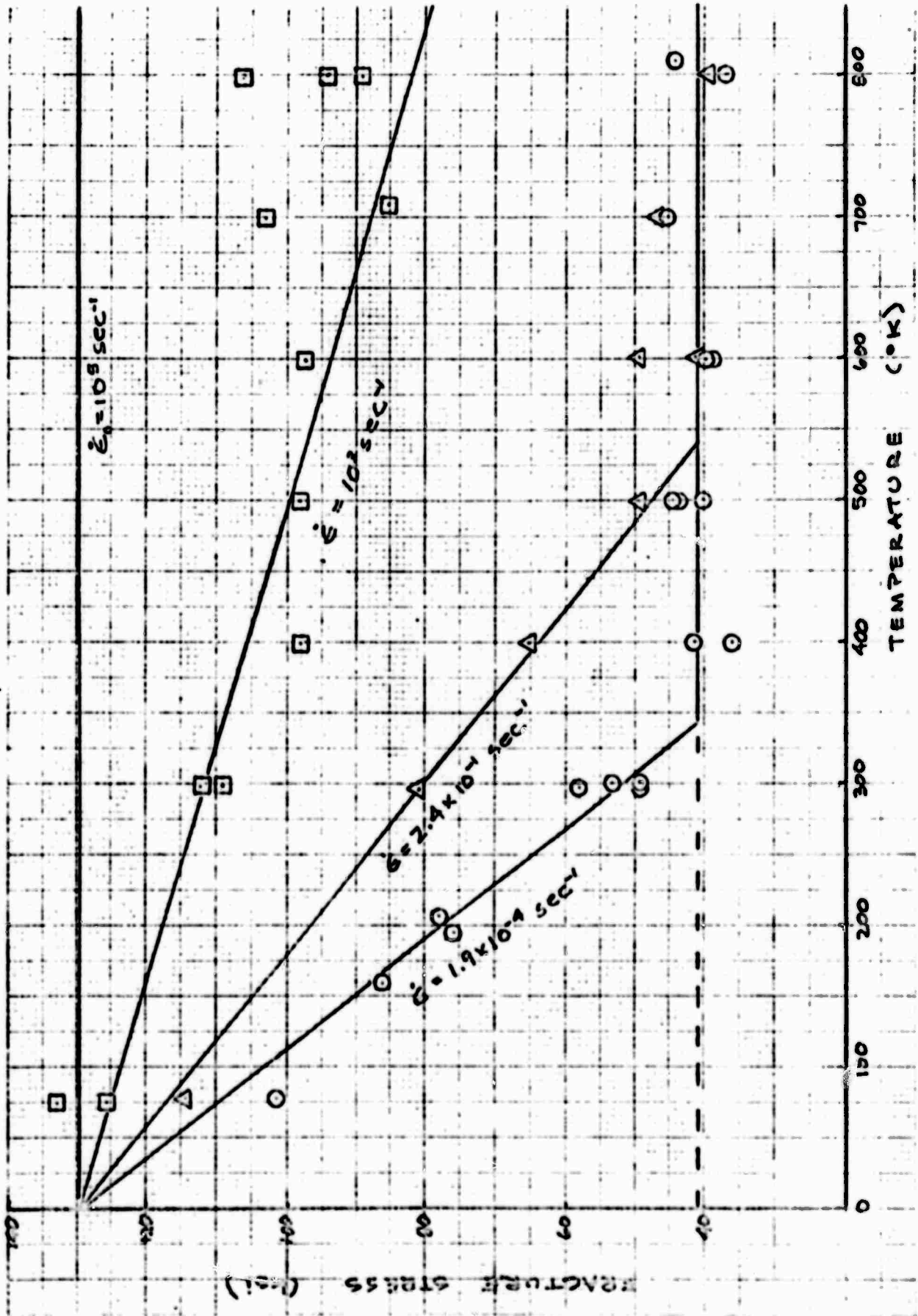


FIGURE 5. EFFECT OF TEMPERATURE AND STRAIN RATE ON FRACTURE STRESS

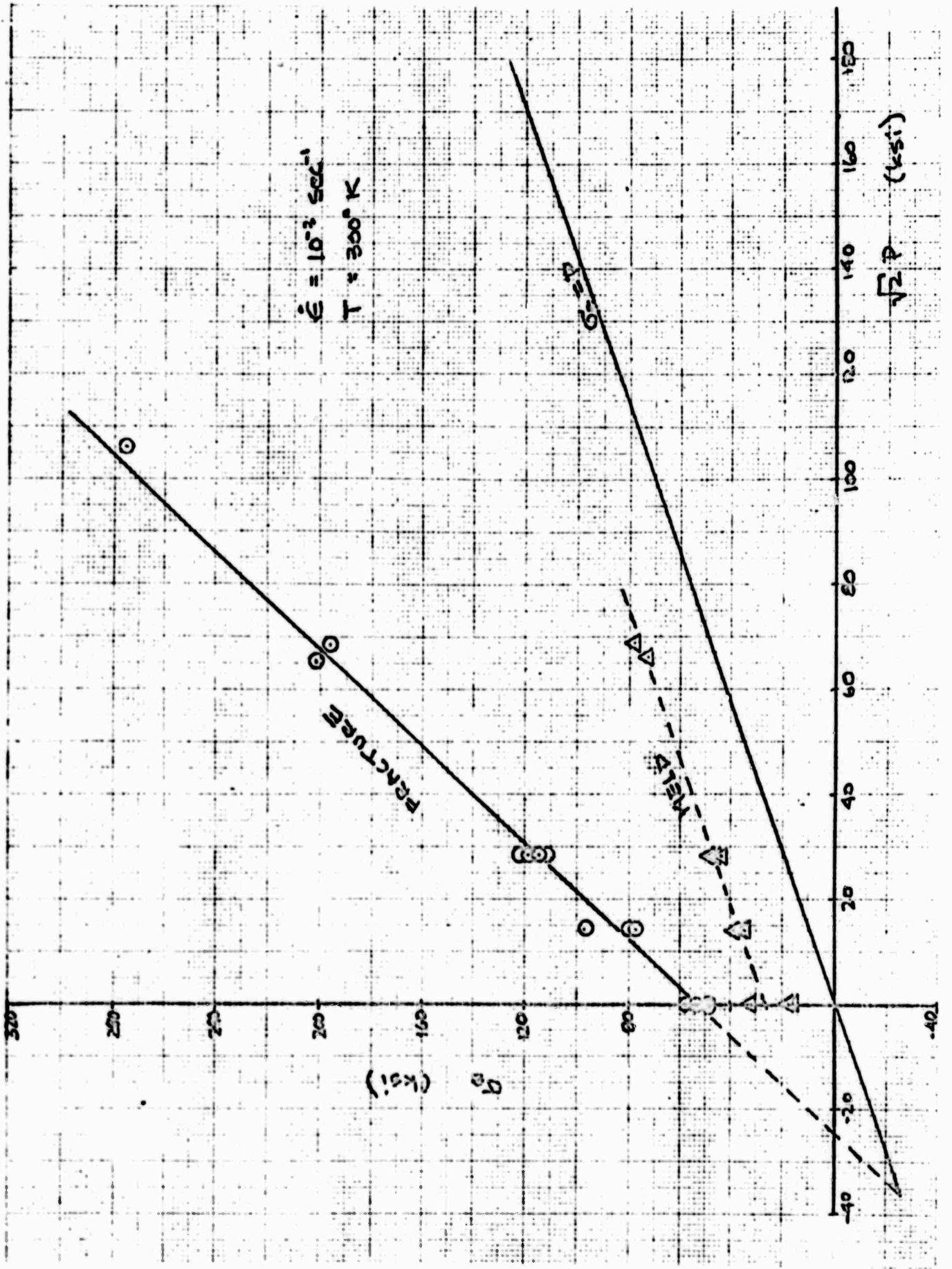


FIGURE 6. EFFECT OF CONFINING PRESSURE ON YIELD AND FRACTURE STRESS

where σ_f is the failure stress for a test conducted at constant strain rate, $\dot{\epsilon}$, and temperature T . σ_0 , ρ and $\dot{\epsilon}_0$ are constants. For the range in parameters studied, the data indicates both a maximum and a minimum stress required to produce fracture. The maximum stress, $\sigma_0 = 130$ ksi, is obtained at $T = 0^\circ\text{K}$ or at $\dot{\epsilon} = \dot{\epsilon}_0 = 10^5 \text{ sec}^{-1}$.

At temperatures above absolute zero, thermal energy is available to assist in both flow and fracture processes, thereby reducing the stress required to produce fracture. Since the thermal contribution is due to random fluctuations, the probability of thermal activation is dependent upon time. The higher the rate of deformation, the lower the thermal contribution and the higher the required stress. The present data indicates a limiting strain rate of 10^5 sec^{-1} . The significance of this rate is difficult to define until we obtain some knowledge of the explicit rate-controlling mechanisms involved. It is not clear at present whether these are crack nucleation mechanisms, perhaps associated with dislocation processes, or the actual rupturing of bonds associated with crack growth.

The data also shows a threshold stress required to initiate fracture of about 40 ksi. At this stress level the fracture process appears to become athermal or independent of either strain rate or temperature.

At the higher temperatures, the Hopkinson bar results at 10^3 sec^{-1} seem to scatter somewhat. This may be explained by the very high strain rate sensitivity in this region. From Equation (1)

$$\frac{d\sigma}{d \ln \dot{\epsilon}} = \beta T \quad (2)$$

For $\beta = 0.029 \text{ ksi}/^\circ\text{K}$ and $T = 800^\circ\text{K}$, a tenfold increase in strain rate results in a $\Delta\sigma$ of 23.2 ksi. The quoted strain rate is obtained by averaging both spatially (length of specimen) and temporally (duration of test). A more detailed analysis of the Hopkinson bar data may yield a better estimate of the stress-time history to failure for these specimens. The effective rates may be higher than initial estimates and account for the apparent scatter.

The pressure dependence of the yield (proportional limit) and fracture strength is shown in Figure 6. This preliminary data indicates very little pressure dependence for the yield strength and a linear dependence for the fracture strength. The data is plotted on a plane in stress space passing through the σ_z axis and the hydrostatic axis ($\sigma_z = P$). All the pressure data plotted were obtained at a single temperature and strain rate. In future work, we will obtain the same yield and fracture boundaries at strain rates up to approximately 10^3 sec^{-1} (Hopkinson bar).

The independence of the yield or elastic limit from pressure would suggest that it is associated with intracrystalline slip processes rather than micro-cracking, as the former is generally pressure independent while the latter should be pressure sensitive. Further study of the volume compressibility, microscopic examination of prefracture and fractured specimens, and other means will be used in an attempt to define the deformation mechanisms leading to gross fracture.



From the data obtained thus far, a coherent picture begins to emerge of the strain rate, temperature, and pressure dependence of basalt in compression. The temperature and strain rate dependence appears to be correlated well by relations of the form [e.g., Eq. (1)] derivable from thermal activation theory. This theory is rather general, however, and has been applied, for example, to the mechanisms of slip or inelastic flow^(1,4), time to failure in creep rupture experiments⁽⁵⁾, and the velocity of crack propagation⁽⁶⁾. Therefore, rather precise knowledge of the controlling mechanisms involved is required in order to transform the empirical coefficients in Eq. (1) into physically meaningful quantities such as activation energy, volume, etc.

The pressure effect appears to follow a linear Coulomb-Mohr relation although additional tests are needed at the higher pressures. Yet to be determined is the interaction between the pressure and temperature or strain rate. The strain-rate tests at pressure should resolve this question. Because of the equivalence shown between strain rate and temperature, the effect of combined elevated temperature and pressure should be predictable.

IV. FUTURE WORK

During the remaining contract period primary effort will be in the following areas:

1. Additional testing, particularly to determine the effect of higher strain rates in combination with confining pressure.
2. Microscopic examination of the fracture surfaces for correlation with the test conditions.

3. Development of constitutive equations. As far as possible, relate these to the physical mechanisms leading to catastrophic fracture of basalt.

There appear to be no significant technical difficulties leading to the successful completion of this work.

V. REFERENCES

1. U. S. Lindholm, "Some Experiments with the Split Hopkinson Pressure Bar," *J. Mech. Phys. Solids*, 12, 317 (1964).
2. U. S. Lindholm and L. M. Yeakley "High Strain Rate Testing: Tension and Compression," *Exp. Mech.*, 8, 1 (1968).
3. S. J. Green and R. D. Perkins, "Uniaxial Compression Tests at Strain Rates from 10^{-4} /sec to 10^4 /sec on Three Geologic Materials," General Motors Report MSL-68-6, (1968).
4. H. C. Heard, "Steady State Flow of Yule Marble at 500-800°C," *Trans. Am. Geophys. Union*, 49, 312 (1968).
5. S. N. Zhurkov and T. P. Sanfirova, "A Study of the Time and Temperature Dependencies of Mechanical Strength," *Soviet Physics-Solid State*, 2, 933 (1960).
6. V. R. Regel and A. M. Leksovskii, "Thermal-Fluctuation Growth of Main-Line Cracks in Polymers," *Soviet Physics-Solid State* 12, 2643 (1971).